RESEARCH ARTICLE

New Poly(butylene succinate)/Layered Silicate Nanocomposites. 1: Preparation and Mechanical Properties

Suprakas Sinha Ray,[a] Kazuaki Okamoto,[b] Pralay Maiti,[a] and Masami Okamoto[a,*]

[a] *Advanced Polymeric Materials Engineering, Graduate School of Engineering, Toyota Technological Institute, Hisakata 2-12-1, Tempaku, Nagoya 468 8511, Japan*

[b] *Nagoya Municipal Research Institute, Rokuban 3-4-41, Atsuta, Nagoya 456-0058, Japan*

New poly(butylene succinate) (PBS)/layered silicate nanocomposites have been successfully prepared by simple melt extrusion of PBS and octadecylammonium modified montmorillonite (C_{18}-mmt) at 150 °C. The d-spacing of both C_{18}-mmt and intercalated nanocomposites was investigated by wide-angle X-ray diffraction analysis. Bright-field transmission electron microscopic study showed several stacked silicate layers with random orientation in the PBS matrix. The intercalated nanocomposites exhibited remarkable improvement of mechanical properties in both solid and melt states as compared with that of PBS matrix without clay.

Keywords: Poly(butylene succinate), Nanocomposite, Intercalation, Mechanical Properties.

1. INTRODUCTION

Recently the development of biodegradable polymeric materials has been a subject of great interest because of their benign properties with respect to the environment. Tremendous amounts and varieties of plastics, notably polyolefins, polystyrene, and poly(vinyl chloride), are currently produced mostly from fossil fuels, consumed and discarded into the environment, ending up as spontaneously *undegradable* wastes. Their disposal by incineration always produces CO_2 and contributes to global pollution, and some but not all of them even release toxic gases. For these reasons, there is a need for the development of "green polymeric materials" that would not involve the use of toxic or noxious components in their manufacture and could be degraded in the natural environment or easily recycled.

Aliphatic polyesters are among the most promising materials for the production of environmentally friendly biodegradable plastics. Biodegradation of aliphatic polyester is well known, in that some bacteria degrade them by producing enzymes, which attack the polymer. One of them is poly(butylene succinate) (PBS) (trade name Bionolle) and is chemically synthesized by polycondensation of 1,4-butanediol with succinic acid. PBS is commercially available as an aliphatic thermoplastic polyester with many interesting properties, including biodegradability, melt processability, and thermal and chemical resistance.[1] PBS has excellent processability, so it can be processed as a textile into melt blow; multifilaments; monofilaments; and nonwoven, flat, and split yarn, and as a plastics into injection-molded products.[2] Although the above properties show potential, the near-future application of PBS, however, has some technical problems, such as softness, low gas barrier properties, etc., to be overcome. In particular, the resin properties have to be improved for individual end-use applications.

In the past few years there has been intense interest in dispersing organically modified layered silicates (OMLS) in polymer matrices, particularly as mechanical reinforcement at low silicate loading levels.[3–12] As a result of their high aspect ratio, the introduction of intercalated or exfoliated OMLS in the polymer matrix can dramatically enhance the mechanical properties[3,7] and decrease gas permeability,[13] and flammability,[14] etc. for various end-use applications. In a natural extension of our earlier work on biodegradable polylactide/layered silicate nanocomposites,[15,16] we have applied this nanocomposite method to another biodegradable polymer PBS. This is the first report in which we will describe the preparation, structure, and mechanical properties of nanocomposites based on PBS and montmorillonite (C_{18}-mmt).

2. EXPERIMENTAL DETAILS

2.1. Materials

The C_{18}-mmt used in this study was supplied by Nanocor, and was prepared by replacing Na^+ in montmorillonite with a cation exchange capacity of 110 meq/100 g with

*Author to whom correspondence should be addressed.

  1533-4880/2002/02/001/006/$17.00+.25 doi:10.1166/jnn.2002.086

octadecylammonium cation by an ion exchange reaction. PBS used in this study is commercial grade (Bionolle: 1012) produced by Showa Denko Co. (Japan) and was dried in an airflow oven prior to use.

2.2. Nanocomposite Preparation

For nanocomposite preparation, C_{18}-mmt (powder form) and PBS (pellet form) were first dry-mixed by shaking them in a bag. The mixture was then melt-extruded with a twin-screw extruder (KZW15-30TGN; Technovel Corp.) operated at 150 °C to yield light gray strands. The compositions of the prepared nanocomposites are presented in Table I. The extruded strands were then palletized and dried under vacuum at 75 °C for 7 h to remove any moisture. (Hereafter, the product nanocomposites are abbreviated as PBSCNs.) The PBSCNs were of two different clay contents (inorganic part) of 1.7 wt.% and 2.8 wt.% (correspondingly abbreviated as PBSCN1.7 and PBSCN2.8, respectively). The nanocomposite pellets were then converted into sheets with a thickness of 0.7–2 mm by pressing with ~1.5 MPa at 135 °C for 3 min. The molded sheets were then quickly quenched between glass plates and then annealed at 60 °C for 1.5 h to crystallize completely before being subjected to all measurements. The contents of the inorganic part in the PBSCNs were measured by burning the PBSCNs sheets at 950 °C in a furnace.

2.3. Characterization Methods

The glass transition temperature (T_g) and the melting temperature (T_m) of the PBS matrix and PBSCNs were determined with a temperature-modulated differential scanning calorimeter (TMDSC) (MDSC, TA2920; TA instruments) operated at a heating rate of 2°/min with a heating/cooling cycle with a modulation period of 60 s and an amplitude of ±0.318 °C. The measured values of T_m and T_g of PBSCNs and PBS are also presented in Table I.

The number-average (M_n) and weight-average molecular weights (M_w) of the PBS matrix (before and after nanocomposite preparation) were determined from gel permeation chromatography (GPC) (HLC-8121; Tosoh Co.) based on the calibration curve of polystyrene standards and chloroform as a carrier solvent at 40 °C, with a flow rate of 0.5 ml/min. The GPC results (Table I) indicate almost no degradation of the PBS matrix after nanocomposite preparation.

Table I. Composition and characteristic parameters of PBSCNs based on PBS and C_{18}-mmt.

Sample	Composition, wt.% PBS	Composition, wt.% C_{18}-mmt[a]	$M_w \times 10^{-3}$ (g/mol)	M_w/M_n	T_g/°C	T_m/°C
PBS	100	—	104	3.90	−30.0	114.0
PBSCN1.7	97	3 (1.7)	96	4.02	−30.5	114.7
PBSCN2.8	95	5 (2.8)	95	4.12	−30.5	115.0

[a] Value in parentheses indicates the percentage of the inorganic part after burning.

Wide-angle X-ray diffraction (WAXD) experiments were performed for the C_{18}-mmt powder, PBSCNs, and PBS matrix with a MXlabo diffractometer (MAC Science Co.), which has an X-ray generator of 3 kW, a graphite monochromator, and CuK_α radiation (wavelength $\lambda = 0.154$ nm) and is operated at 40 kV/20 mA. The samples were scanned at 2°/min under a diffraction angle of 2Θ in the range of 1–70°.

To investigate the nanoscale structure of the PBSCNs, a transmission electron microscope (TEM) (H-7100; Hitachi Co.) was also used and operated at an accelerating voltage of 100 kV. Ultrathin sections with a thickness of 100 nm were microtomed at −80 °C with a Reichert Ultracut Cryoultramicrotome without staining. The TEM photographs were taken from the edge of the compression-molded sheet.

Dynamic mechanical properties of PBSCNs and the corresponding PBS matrix were measured with a Rheometrics Dynamic Analyzer (RDAII) in the tension–torsion mode. The experiments on the temperature dependence of dynamic storage modulus (G'), loss modulus (G''), and their ratio, $\tan\delta$, were conducted at a constant frequency (ω) of 6.28 rad/s with a strain amplitude of 0.05% and in the temperature range of −50 °C to 110 °C with a heating rate of 2°/min.

Rheological measurements of the molten state were also performed on RDAII instruments with a troque transducer capable of measurements over the range of 0.2–2000 g · cm. Dynamic oscillatory shear measurements were performed with a set of 25-mm-diameter parallel plates with a sample thickness of 1–2 mm and in the temperature range of 115–155 °C. The strain amplitude was fixed at 5% to obtain reasonable signal intensities even at elevated temperatures or low ω to avoid the nonlinear response. For each PBSCN investigated the limits of linear viscoelasticity were determined by performing strain sweeps at a series of fixed ω's. The master curves were generated by using the principle of time-temperature superposition, and a common reference temperature (T_{ref}) of 125 °C was chosen as the most representative processing temperature for PBS.

3. RESULTS AND DISCUSSION

The structure of the PBSCNs has typically been elucidated with TEM and WAXD. TEM allows a qualitative understanding of the internal structure through direct visualization. On the other hand, WAXD offers a convenient method of determining the interlayer spacing of the clay layers in the original clay and in the intercalated polymer/clay nanocomposites. Figure 1 shows the results of WAXD patterns of C_{18}-mmt powder, PBSCNs, and PBS matrix in the range of $2\Theta = 1$–10°. The mean interlayer spacing of the (001) plane ($d_{(001)}$) for the C_{18}-mmt

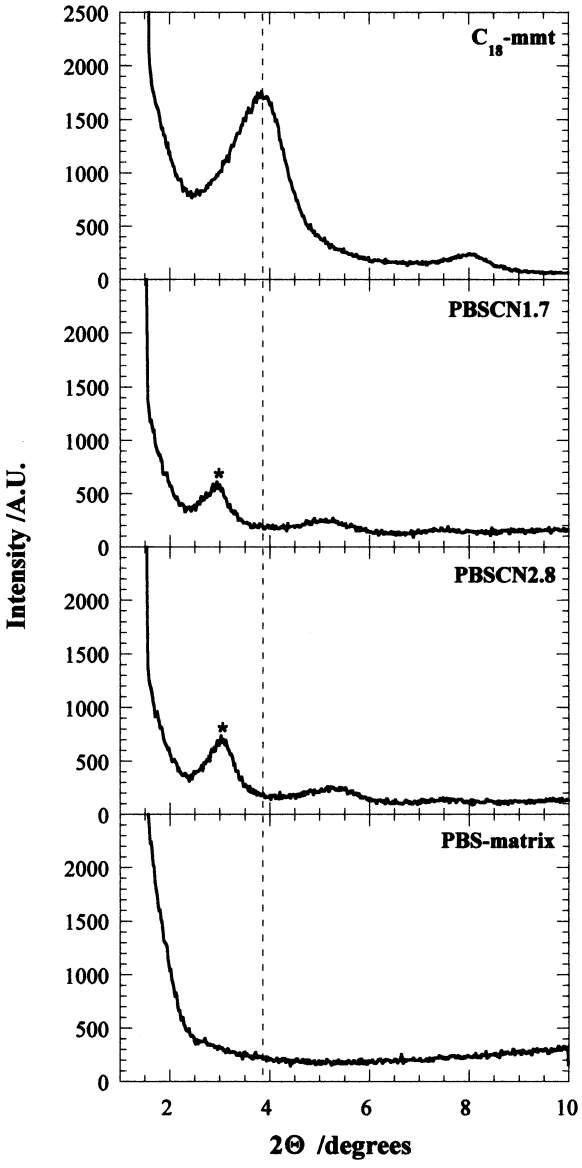

Fig. 1. WAXD patterns for C_{18}-mmt, PBSCNs and PBS respectively. The dashed line indicates the location of the silicate (001) reflection of C_{18}-mmt.

powder obtained by WAXD measurements is 2.31 nm ($2\Theta \cong 3.82°$). The pattern of the PBS matrix is displayed as a baseline to compare the existence of diffraction peaks coming from the C_{18}-mmt dispersed in the polymer matrix. For PBSCN1.7, a clear peak is observed at $2\Theta \cong 2.92°$, and a very small peak is observed at $2\Theta \cong 5.14°$, corresponding to (001) and (002) planes of the silicate layers dispersed in the PBS matrix. In the case of PBSCN2.8, both peaks become strong and are shifted toward the higher angle. The difference in the interlayer spacing between the C_{18}-mmt powder and that in PBSCNs after melt mixing is presumably due to the intercalation of the PBS chains into the silicate galleries. The existence of a sharp Bragg peak in PBSCNs shows that the dispersed

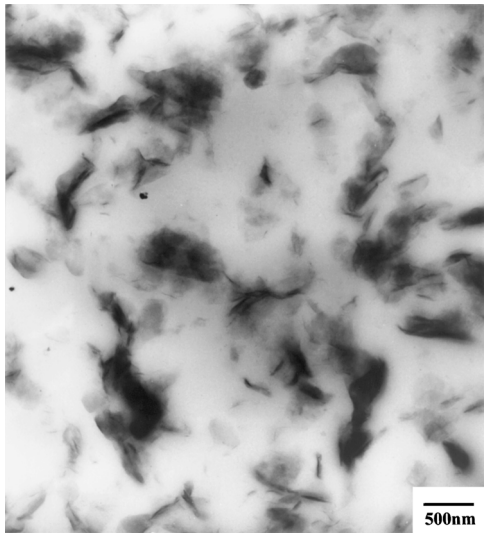

Fig. 2. TEM micrograph of PBSCN2.8.

clay particles in the PBSCNs retain an ordered structure after melt extrusion.

Figure 2 shows the TEM bright-field image of the PBSCN2.8 shown in the WAXD pattern of Figure 1, in which dark entities are the cross section of the stacked and intercalated organically modified silicate layers. From the TEM image, we observed stacked and flocculated silicate layers, which are randomly distributed in the PBS matrix. The size of some of the stacked-silicate layers appears to reach about 300–700 nm. However, we cannot estimate the thickness precisely from the TEM image.

Figure 3 shows the temperature dependence of G', G'', and $\tan\delta$ of the intercalated PBSCNs and the corresponding PBS matrix. The enhancement in moduli appears in different magnitudes at various temperature ranges for all PBSCNs. Below T_g, the enhancement of G' is clear in the intercalated PBSCNs. In the temperature range of -50 °C to -30 °C, the increments in G' are 33% for PBSCN1.7 and 62% for PBSCN2.8 as compared with that of the PBS matrix. Furthermore, in the temperature range of 30 °C to 100 °C, both PBSCNs exhibited higher enhancement of G' as compared with that of matrix without clay. At room temperature, PBSCN2.8 showed a higher increment in G' of 82%, whereas that of PBSCN1.7 was only 42% than that of the PBS matrix.

For PBSCNs, the enhancement tendency of G' with temperature is almost identical to that of well-established intercalated polypropylene/montmorillonite nanocomposites[11] and to that of nearly exfoliated nylon6/montmorillonite nanocomposites.[7, 10] For these systems, there is a maximum 40–50% increment of G' compared with that of the matrix well below T_g, and above T_g there is a strong enhancement (>100%) of G'. This behavior is common for reported nanocomposites, and the reason for this is the strong reinforcement effect of the clay particles above T_g when materials become soft.

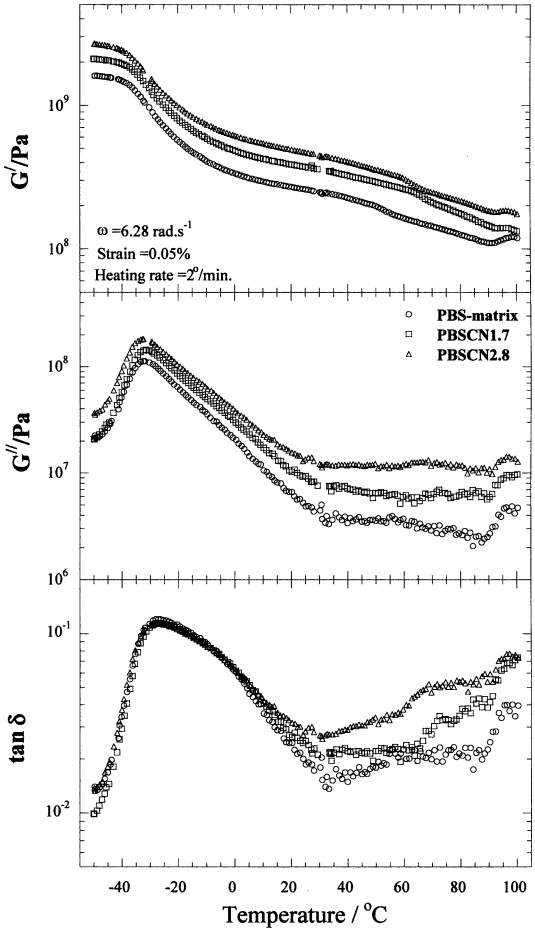

Fig. 3. Temperature dependence of G', G'' and $\tan\delta$, for PBSCNs and the corresponding PBS-matrix.

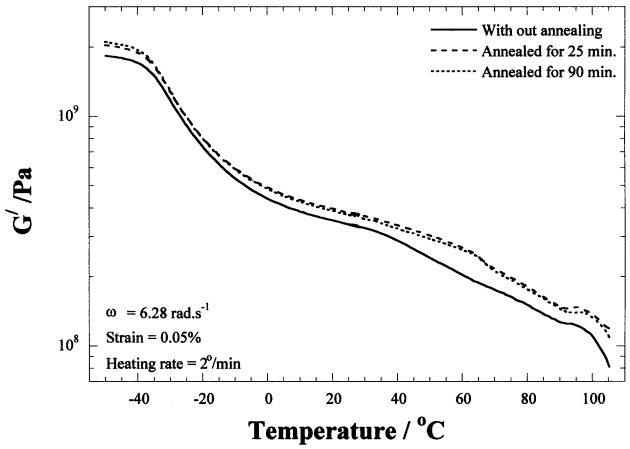

Fig. 4. Temperature dependence of G' for PBSCN1.7 samples annealed at 60 °C for three different time.

However, in the case of PBSCNs, the order of enhancement of G' is almost the same below and above T_g, and this behavior may be due to the extremely low T_g (−30 °C) of the PBS matrix.

The presence of clay particles in the matrix does not lead to a big shift and broadening of the $\tan\delta$ curves for both nanocomposites. However, there is a large enhancement of both $\tan\delta$ and G'' for the PBSCNs above T_g in comparison with that of PBS matrix. This is caused by the large anisotropy of the dispersed clay particles due to flocculation.

We may expect the mechanical properties of PBSCNs to change significantly as a function of annealing condition. Accordingly, we measured the temperature dependence of G' for PBSCN1.7 samples annealed at 60 °C for three different times, as shown in Figure 4. Generally, annealing is necessary to ensure the complete crystallization of the sample before being subjected to all measurements because mechanical and other properties directly depend upon the crystallization.[17] It is clear from Figure 4 that, for a particular temperature, G' increases with increasing annealing time; however, G' shows almost the same value for the samples which were respectively annealed for 25 min and 190 min. This is due to the fact that 25 min at 60 °C is enough for PBSCN1.7 to crystallize completely, even though we annealed the samples at 60 °C for 1.5 h to avoid any ambiguity.

Figure 5 shows the plots of reduced angular frequency, $a_T\omega$ versus $G'(\omega)$, $G''(\omega)$, and $(|\eta^*|(\omega))$, respectively, for PBSCNs and PBS matrix. Both $G'(\omega)$ and $G''(\omega)$ exhibit a monotonic increase with increasing clay content at all ω's. The terminal zone dependence of $G'(\omega)$ and $G''(\omega)$ shows terminal behavior of ordinary polymer melts ($G'(\omega) \propto \omega^2$ and $G''(\omega) \propto \omega$) for PBS, but nonterminal behavior appears in the cases of PBSCN1.8 and PBSCN2.8. In the terminal zone of the polymer/OMLS nanocomposites, the curves can be expressed by power-law dependencies of both $G'(\omega)$ and $G''(\omega)$.[18] Terminal zone slopes are estimated at lower ω region (<10 rad/s) and are presented in Table II. The lower slope values and the higher absolute values of the dynamic moduli indicate the formation of spatially linked structure in the PBSCNs in the molten state.[15, 19]

Because of this structure or highly geometric constraints, the relaxation of the structure with low ω (<10 rad/s) is partially prevented and leads to a very high viscosity for PBSCN2.8 as compared with that of PBS ($|\eta^*|(\omega)$ vs. $a_T\omega$).

The temperature dependence frequency shift factors (a_T, WLF type)[20] used to generate master curves shown in Figure 5 are shown in Figure 6. The complete independence of the frequency shift factors from the silicate loading suggests that the temperature-dependent relaxation processes observed in the viscoelastic measurements are essentially unaffected by the presence of the silicate layers in the case of weak interaction between silicate layers and polymer matrix.[21]

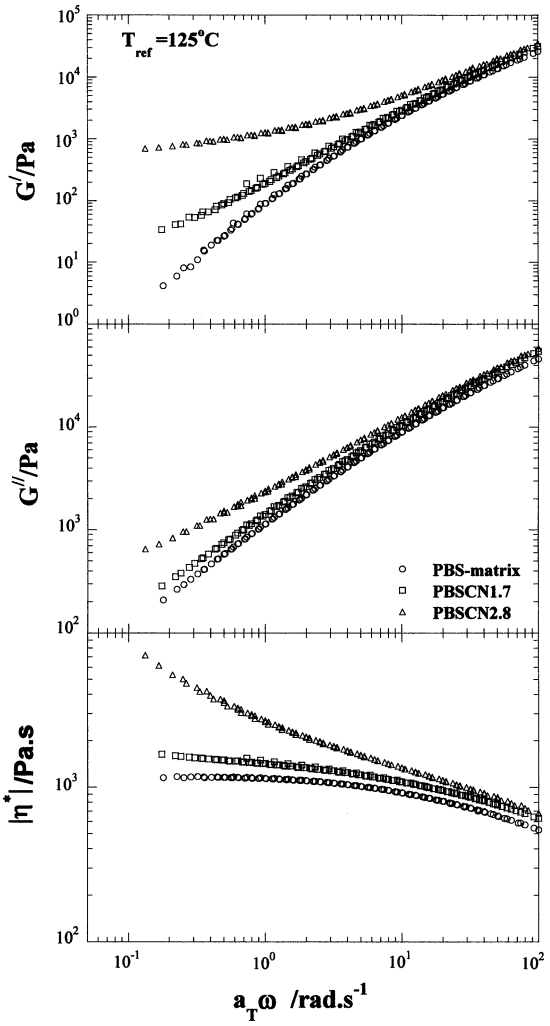

Fig. 5. Reduced frequency dependency of $G'(\omega)$, $G''(\omega)$, and $[|\eta^*|(\omega)]$ of PBSCNs and PBS-matrix. $T_{ref} = 125$ °C.

Table II. Terminal slopes of G' and G'' vs. $a_T\omega$ for PBS and PBSCNs.

Sample	G'	G''
PBS	1.5	0.9
PBSCN1.7	1.0	0.8
PBSCN2.8	0.3	0.5

4. CONCLUSIONS

We have prepared PBS/mmt nanocomposites by melt extrusion of PBS and C_{18}-mmt, wherein silicate layers of the C_{18}-mmt were intercalated and randomly distributed in the PBS matrix. These systems were the first successful intercalated PBS/mmt nanocomposites. All nanocomposites exhibited remarkable improvement of mechanical properties in both solid and melt states compared with the matrix without clay. In our forthcoming papers,[22] we will describe the preparation of PBSCNs with various types of OMLS. Then we will describe the effect of surfactants and the nature of layered silicates in PBSCNs by focusing on three major aspects: morphological analysis, mechanical property measurements, and rheological properties of PBSCNs. The concurrent improvement of material properties, such as biodegradability, gas barrier properties, and heat distortion temperature, of these nanocomposites will also be reported.

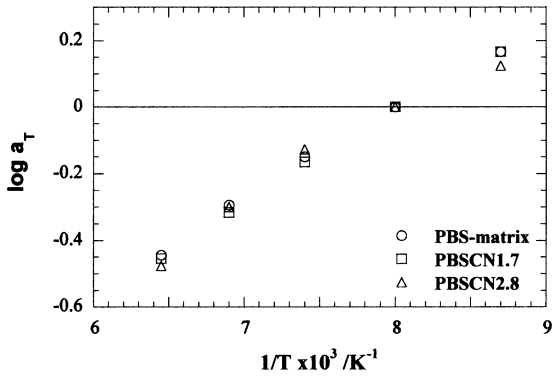

Fig. 6. Frequency shift factors (a_T) as a function of temperature for PBS and PBSCNs.

Acknowledgments: The present work was partially supported by a Grant-in-Aid for the Academic Frontier Center under the project "Future Data Storage Materials," granted by the Ministry of Education, Science, Sports and Culture (1999–2003), Japan.

References and Notes

1. J. A. Ratto, P. J. Stenhouse, M. Auerbach, J. Mitchell, and R. Farrell, *Polymer* 40, 6777 **(1999)** and references cited therein.
2. T. Fujimaki, *Polym. Degrad. Stab.* 59, 209 **(1998)**.
3. P. B. Messersmith and E. P. Giannelis, *Chem. Mater.* 6, 1719 **(1994)**.
4. K. Yono, A. Usuki, T. Kurauchi, and O. Kamigaito, *J. Polym. Sci., Part A: Polym. Chem.* 31, 2493 **(1993)**.
5. P. B. Messersmith and E. P. Giannelis, *J. Polym. Sci., Part A: Polym. Chem.* 33, 1047 **(1995)**.
6. P. C. LeBaron, Z. Wang, and T. Pinnavaia, *J. Appl. Clay Sci.* 15, 11 **(1999)**.
7. E. P. Giannelis, R. Krishnamoorti, and E. Manias, *Adv. Polym. Sci.* 138, 107 **(1999)**.
8. M. Alexander and P. Dubois, *Mater. Sci. Eng.* 28, 1 **(2000)**.
9. M. Okamoto, P. H. Nam, P. Maiti, T. Kotaka, N. Hasegawa, and A. Usuki, *NanoLett.* 1, 295 **(2001)**; M. Okamoto, P. H. Nam, P. Maiti, T. Kotaka, T. Nakayama, M. Takada, M. Ohshima, A. Usuki, N. Hasegawa, and H. Okamoto, *NanoLett.* 1, 503 **(2001)**.
10. A. Usuki, M. Kawasumi, Y. Kojima, A. Okada, T. Kurauchi, and O. Kamigaito, *J. Mater. Res.* 14, 1174 **(1993)**.
11. P. H. Nam, P. Maiti, M. Okamoto, T. Kotaka, N. Hasegawa, and A. Usuki, *Polymer* 42, 9633 **(2001)**.
12. R. A. Vaia and E. P. Giannelis, *Macromolecules* 30, 8000 **(1997)** and references cited therein.
13. K. Yano, A. Usuki, A. Okada, T. Kurauchi, and O. Kamigaito, *J. Appl. Polym. Sci.* 31, 2493 **(1993)**.
14. J. W. Gilman, T. Kashiwagi, and J. D. Lichtenhan, *SAMPE J.* 33, 40 **(1997)**; J. W. Gilman, C. L. Jackson, A. B. Morgan, R. H. Jr, E. Manias, E. P. Giannelis, M. Wuthenow, D. Hilton, and S. H. Phillips, *Chem. Mater.* 12, 1866 **(2000)**.

15. S. Sinha Ray, P. Maiti, M. Okamoto, K. Yamada, and K. Ueda, *Macromolecules*, in press; S. Sinha Ray, K. Okamoto, K. Yamada, and M. Okamoto, *NanoLett.*, in press.
16. S. Sinha Ray, M. Okamoto, and K. Yamada, unpublished observations.
17. P. Maiti, P. H. Nam, M. Okamoto, N. Hasegawa, and A. Usuki, *Macromolecules*, in press.
18. J. Ren, A. S. Silva, and R. Krishnamoorti, *Macromolecules* 33, 3739 (**2000**).
19. A. Eckstein, Chr. Friedrich, A. Lobbrecht, R. Spitz, and R. Mulhaupt, *Acta Polym.* 48, 41 (**1997**).
20. M. L. Williams, R. F. Landel, and J. D. Ferry, *J. Am. Chem. Soc.* 77, 3701 (**1955**).
21. R. Krishnamoorti and E. P. Giannelis, *Macromolecules* 30, 4097 (**1997**).
22. S. Sinha Ray, K. Okamoto, and M. Okamoto, unpublished observations.

Received: 14 December 2001. Revised/Accepted: 19 February 2002.